

Design and Development of a Novel High Resolution Absolute Rotary Encoder System Based on Affine n-digit N-ary Gray Code

Sarbajit Paul* and Junghwan Chang[†]

Abstract – This paper presents a new type of absolute rotary encoder system based on the affine n-digit N-ary gray code. A brief comparison of the existing encoder systems is carried out in terms of resolution, encoding and decoding principles and number of sensor heads needed. Using the proposed method, two different types of encoder disks are designed, namely, color-coded disk and grayscale coded disk. The designed coded disk pattern is used to manufacture 3 digit 3 ary and 2 digit 5 ary grayscale coded disks respectively. The manufactured disk is used with the light emitter and photodetector assembly to design the entire encode system. Experimental analysis is done on the designed prototype with LabVIEW platform for data acquisition. A comparison of the designed system is done with the traditional binary gray code encoder system in terms of resolution, disk diameter, number of tracks and data acquisition system. The resolution of the manufactured system is 3 times higher than the conventional system. Also, for a 5 digit 5 ary coded encoder system, a resolution approximately 100 times better than the conventional binary system can be achieved. In general, the proposed encoder system gives $(N/2)^n$ times better resolution compared with the traditional gray coded disk. The miniaturization in diameter of the coded disk can be achieved compared to the conventional binary systems.

Keywords: Absolute encoder, N-digit N-ary gray code, Color-coded disk, Grayscale disk, Encoder design

1. Introduction

Rotary optical encoder plays various important roles in the automation industry, radar system, and high-performance servo applications. It is an electromechanical device that can convert real-time feedback information about the angular or linear position into numerical codes. The rotary encoders can be classified into incremental and absolute encoders. Incremental encoders contain simple encoder disk with alternate black and transparent patterns over a single track circular disk. Using an incremental encoder, the real time absolute position information cannot be achieved. This drawback of the incremental encoder can be overcome using absolute encoders. Absolute encoder employs multiple track disk with different cyclic numeric codes [1].

In the case of absolute encoder, using the binary or gray code pattern disk, the real-time angular position information can be converted into unique numerical codes. These detected codes can then be converted back to user readable data by the decoder assembly in the data acquisition circuit. Although absolute encoders are one of the most frequently used sensors in factory automation

system, these encoders suffer from the inherent problem of quantization noise on account of the limited resolution they possess [2]. The resolution of the binary gray coded absolute encoder is directly proportional to the number of the disk tracks and the cost. The resolution can be improved by increasing the number of the tracks in the coded disk. With the increase of the number of tracks, the size and weight of the encoder system increase simultaneously. This eventually increases the cost of the overall system. Due to the high market demand of the absolute encoders and the limitations the traditional optical encoders possess, many researchers are working on the topic of design of a high precision and miniaturized optical encoder that can substitute the already existing encoder systems.

A number of studies have been performed since last two decades to achieve the goal to design a high resolution and miniaturized encoder system. Hua *et al.* proposed single track disks to reduce the number of coded tracks of the encoders [3]. Some researchers have used pseudorandom coded patterns [4] or De Burjijn sequence [5] to design the coded track. Also, M-code was used to design the absolute encoder disk pattern [6]. These methods use single coded track encoder disk to find the position. Coded track design based on the graph theory was proposed by T. Dziwinski [7]. The graph theory based track design uses two-dimensional matrix decoding by the use of two-dimensional image sensors.

This paper deals with a new coded disk design method

[†] Corresponding Author: Mechatronics System Research Laboratory, Dept. of Electrical Engineering, Dong-A University, Korea. (cjhwan@dau.ac.kr)

* Mechatronics System Research Laboratory, Dept. of Electrical Engineering, Dong-A University, Korea. (spaul@donga.ac.kr)

Received: March 23, 2017; Accepted: September 27, 2017

that can be used to realize a high resolution compact absolute optical encoder. Earlier documented research works have used binary coding systems. In a binary coding system, the base term of the denominator of the resolution expression for encoder system is always fixed to two. The main focus of the proposed work is to change both the base and power terms of the denominator in resolution expression of the encoder. To fulfill this goal, the proposed method has employed n -digit N -ary gray code. the n -digit N -ary gray code is widely used in many areas of communication and computer applications. Raymond *et al.* describe the use of N -ary gray code in the field of digital circuit design [8]. The N -ary gray code is used in digital communication system frequently [9-12]. In [13], the N -ary gray code was used for image bit plane decomposition, image denoising, and encryption. Motion estimation of video processing has also used N -ary gray codes [14]. The N -ary gray code can be divided into different types depending on their characteristics. C. Savage has documented different types of N -ary gray codes in [15]. All the available N -ary gray codes cannot be used to design the absolute rotary encoder disk to measure angular position. The N -ary gray code must follow the basic criteria of bijection and cyclic characteristics to be used in optical encoder disk design. This paper considers cyclic n -digit N -ary gray code based on affine transformation to meet the above mentioned conditions. The use of cyclic n digit N -ary gray code to code the encoder disk opens the option to change not only the power but also the base of the denominator in the encoder resolution expression. This results in the improvement of the resolution of the absolute encoder. In addition to that, miniaturization in the overall track diameter can be achieved compared to the traditional binary encoder systems. Even though the coded disk uses same numbers of tracks and sensors as that of the traditional binary gray coded encoder disk of same size and diameter, the resolution is higher than the traditional binary gray coded encoder. Also, the comparison with other encoder systems shows that by using the proposed method both miniaturization in disk design and high resolution can be achieved simultaneously.

The whole paper is divided into six sections, namely: section 2 describes the brief overview of the existing encoder systems and comparison in terms of resolution, encoding and decoding principles; section 3 describes in detail the section criteria of the proposed method and the mathematical derivation behind it; section 4 deals with the encoding and decoding method with physical realization of the disk design; in section 5 the experimental analysis of the designed prototype is studied. Finally, section 6 presents the conclusion.

2. Study of the Existing Absolute Encoder System

An absolute encoder system is shown in Fig. 1. The

Table 1. Comparison among different existing encoder systems

Codes	Gray	Gray with Vernier	M code	Directed graph theory
Expression (Resolution)	$\frac{360^\circ}{2^n}$	$\frac{360^\circ}{2^{n-1}(2^{n-1}-1)}$	$\frac{360^\circ}{2^n}$	$\frac{360^\circ}{2^{N^2}}$
No. of tracks	n	n	1	N^a
No. of sensors	n	$(n-1)+(2^{n-1}\pm 1)$	n	$N \times N$

^a N is the row and column of the $N \times N$ matrix

encoder system is composed of three different sections, namely, the coded disk, the light source, and the photo-detector assembly. As shown in Fig. 1, the coded disk has 3 tracks. For three tracks of the coded disk, three light sources and three photodetectors are needed. In general, for encoders using the binary gray code, to achieve n bits of resolution, n numbers of coded tracks are needed. To decode n coded tracks, n numbers of sensor heads are required. Optical absolute encoder disk is constructed using cyclic code theory. There are various cyclic coding approaches to encode the coded track. Among all the different kinds of encoder disk coding approaches, disk design based on the binary gray code is the most common one. Fig. 1 presents different coded disk patterns, realized using different cyclic codes. Table 1 shows a comparison among different absolute encoder coding methods. The brief discussion of each disk patterns is as follows,

2.1 Binary gray coded encoder disk

In 1953, F. Gray proposed the reflected gray code. The arrangement of 3 bits coded track absolute encoders is shown in Fig. 1(a). The small red circles on the coded disk design in Fig. 1 are the position for the photo sensor modules used to sense the coded pattern. The design of the coded disk, encoding and decoding are simple in gray code based system. But the main drawback of the gray code based system is, to achieve n bits of resolution, n numbers of coded tracks are needed. To decode n coded tracks, n numbers of sensor heads are required. So the high-resolution system can only be realized at the expense of the big size and the high cost.

2.2. Gray coded encoder disk with vernier track

To improve the resolution of the gray code encoder, Wekhande *et al.* used Vernier principle over the traditional binary gray coded track [2]. According to the Vernier principle, n divisions of the Vernier scale have the same length as $n-1$ divisions of the main scale. To apply Vernier principle on the n track gray coded disk, an extra track with 2^n slits are added on the outermost track. Fig. 1(b) shows the Vernier track gray coded absolute encoder. Compared with the traditional gray coded track disk, the addition of Vernier track improves the resolution greatly. But as shown in Table 1, to detect the whole system we need $2^{n-1} \pm 1$

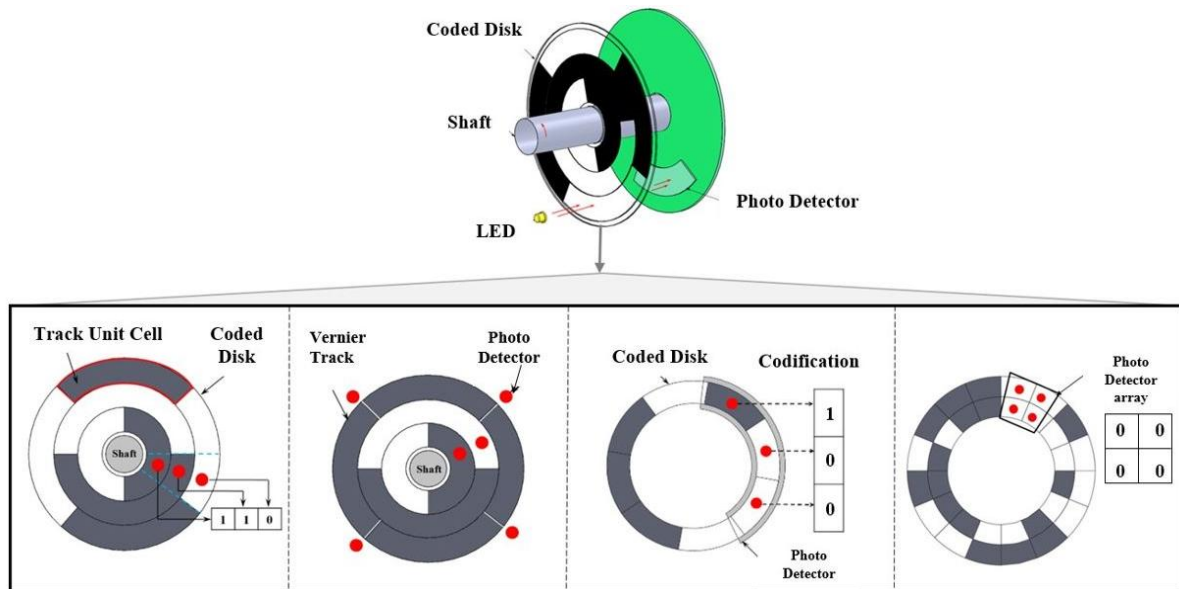


Fig. 1. Traditional encoder system with different coded disk designs (a) gray coded disk (b) gray code disk with Vernier track (c) M-coded disk and (d) Coded disk with graph theory

extra light source and photodetector assembly. This again increases the size and weight of the overall system due to mechanical tolerance to accommodate all the sections.

2.3. M-coded disk

M sequence or maximum length sequence is a pseudorandom binary sequence. The bit pattern in M-code is generated using linear feedback registers [6].

Fig. 1(c) shows a 3-bit M-coded track disk to decode absolute position. As shown in Fig. 1(c), using the M-coded track, single track disk can be designed but to decode n bit M-coded track, n numbers of sensor heads facing parallel to the track are needed. Also, the single track disk has tracks at its outermost periphery. Therefore, in terms of mechanical design, the disk size increases with the increase of the number of bits because the patterns can only be accommodated at the outermost track.

2.4. Graph theory based coded disk

The concept of this coding approach is to find the Hamiltonian cycle in the set of $N \times N$ matrices [7]. The code pattern using this method is shown in Fig. 1(d). As shown in Fig. 1(d), the sensors are assembled in $N \times N$ matrix form. The design of the disk pattern using the graph theory approach gives significant improvement in the resolution. But to code $N \times N$ matrices, N numbers of tracks are needed. Also, each track is divided into 2^{N^2} numbers of unit cells. During manufacturing, a minimum mechanical limit in diameter must be followed to accommodate all the unit cell patterns evenly over the circular track. After coding the first track with 2^{N^2} number of unit cell patterns over the minimum diameter, rest of

the $N-1$ tracks with 2^{N^2} unit cell patterns each must be placed over the first track. This causes the divergence of the coding track.

The overview of the existing methods shows that the works are done to improve the resolution of the overall system. But the existing systems did not consider the size of the disk into account. As a result, a miniaturized optical encoder with high resolution cannot be obtained using the above-mentioned disk designs. A different and more efficient coding method is needed that can be used to design a high resolution miniaturized optical encoder.

3. Proposed Method and The Disk Design

To achieve the goal mentioned in section 2, an n -digit N -ary code based disk design method is proposed in this paper. Unlike the binary approach in which the base term is fixed to 2, in n digit N -ary gray code, the base number as well as the exponent of the power representation of the denominator in resolution can be varied. But n -digit N -ary gray code must fulfill the requirement of being a) a bijective and b) cyclic code, to be considered for encoder disk design. The requirements are checked mathematically as follows,

3.1. Algorithm to generate cyclic n -digit N -ary gray code

Step 1 : Check of bijection and lee distance

In the case of n -digit N -ary gray code, for N , $n \geq 2$, an n -digit N -ary gray code is a sequence in which each n digit string with digits from the set $\{0, 1, \dots, N-1\}$ occurs only once [16]. Thus n -digit N -ary gray code satisfies bijection

principle.

The cyclic characteristic of any code or string can be determined by Lee distance or Hamiltonian cycle. The distance between two strings x_1, x_2, \dots, x_n and y_1, y_2, \dots, y_n of equal length n over an N -ary alphabet $\{0, 1, \dots, N-1\}$ of size $N \geq 2$ is called as Lee distance. Mathematically Lee distance is defined as D_L as follows,

$$D_L(x_1, \dots, x_n, y_1, \dots, y_n) = \sum_{i=1}^n \min\{|x_i - y_i|, N - |x_i - y_i|\} \quad (1)$$

Definition 1: If the Lee distance between the last and the first string is equal to 1 bit, the code is called cyclic code.

As mentioned above, in N -ary gray code consecutive strings has Lee distance equals to 1 bit. Thus N -ary gray code is a cyclic code and satisfies bijection. From the above discussion, it is clear that N -ary gray code can be used to design an absolute rotary encoder to measure angular position.

Step 2 : Encoding using Affine transformation

To design the coded disk using the n -digit N -ary gray code, affine transformation method is considered [17-20]. Unlike the other gray code transformation method, this method does not depend on constrain conditions of N to be prime for achieving cyclic code.

A transformation f on the plane of a form $f(x) = Ax + b$ is called an affine transformation, where A is an invertible matrix and b is a constant vector.

Unlike a binary system which deals with 0 and 1, an n -

digit N -ary system or a vector of integers needs a permutation operation P that arranges the n digits from the sequence of vectors $\{0, 1, \dots, N^n-1\}$ in such a way that it generates a cyclic gray code like traditional gray code. Using the affine transformation, a permutation matrix is generated as follows,

$$P = ((I - Z) \cdot V \cdot Q) + u \quad (2)$$

Where Z is an upper diagonal matrix with all its upper diagonal elements 1, u is any $1 \times n$ N -ary vector; S is an $n \times n$ matrix with 1's on its super-diagonal and 0 elsewhere; V is an $n \times n$ matrix with 1's and -1's in its diagonal elements; Q is an $n \times n$ permutation matrix with elements present only on the diagonal. A detail description of the mathematical derivation and the examples are mentioned by the authors in [21]. Fig. 2 presents a flowchart of the encoding process of the n -digit N -ary cyclic gray code.

3.2. Physical circuit to design the code work and the disk prototype

Physically, the code word can be designed using multiplier and adder circuits as shown in Fig. 3(a). Using Fig. 3(a), 3 digit 3 ary gray code can be achieved. The triplets mentioned in the Fig. 3(a) are equivalent to the BCD code in case of a binary system of representation. The bits are generated in the order of MSB to LSB. The generated 3 digit 3 ary gray codes from the corresponding triples are presented in Table 2. As shown in Table 2, each code word combinations designed using the set $\{0, 1, 2\}$ appears only once and the difference between two consecutive code words is 1 bit. Thus the generated 3 digit 3 ary gray code thus obtained, fulfils the requirements mentioned in section 3. A color code equivalent of the generated code is designed using three basic colors red, green and blue. Red, green and blue are considered as 0, 1, and 2 respectively. The color codes are presented in Table 2.

The 3 digit 3 ary color codes can be arranged over a disk as shown in Fig. 3(b). In terms of angular distance, the 3 digit 3 ary color code can divide 360° into 27 distinct divisions. The expression of the gray code in the Table 1 can be modified in terms of n -digit N -ary code as follows,

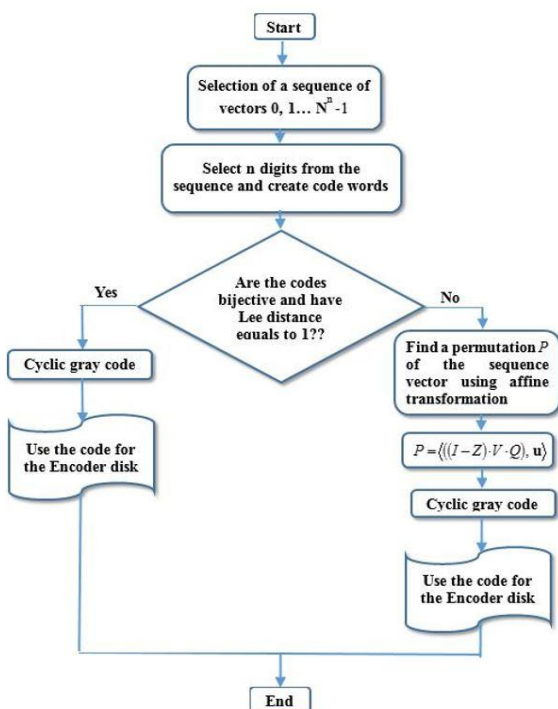


Fig 2. Flowchart for the generation of the affine n -digit N -ary gray code

Table 2. Encoded N -ary gray code and color code

Decimal	Triple	Ternary cyclic gray code	Color code
0	000	000	RRR
1	001	001	RRG
2	002	002	RRB
3	010	012	RGB
.	.	.	.
23	212	221	BBG
24	220	201	BRG
25	221	202	BRB
26	222	200	BRR

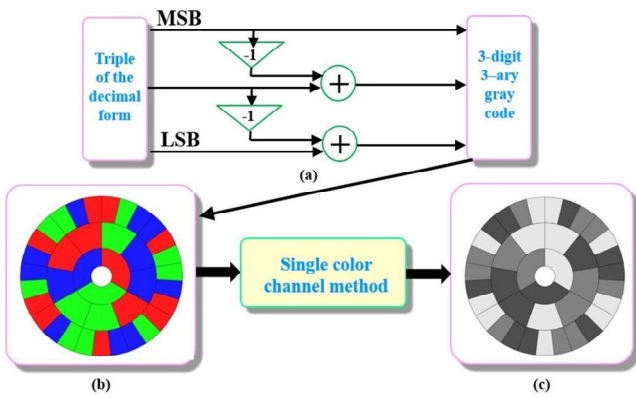


Fig 3. (a) Encoding principle (b) Color 3 digit 3 ary gray code (c) Color 3 digit 3 ary gray code in gray scale, generated with single channel method

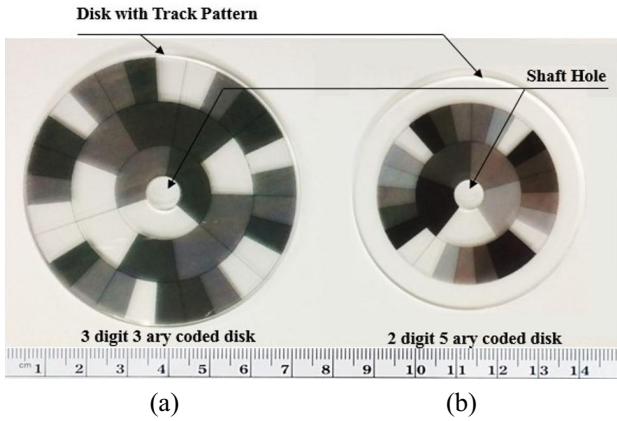


Fig 4. The prototype of (a) 3 digit 3 ary gray scale disk and (b) 2 digit 5 ary gray scale disk

$$\text{Resolution} = \frac{360^\circ}{N^n} \quad (3)$$

Another version of the color-coded disk can be obtained by grayscale color conversion of the color-coded disk shown in Fig.3(c). The grayscale color disk can be obtained by passing the RGB colored disk through the single color channel as shown in Fig.3. The single color channel method is a grayscale conversion method that uses the data from a single color channel. In Fig.3, the red color channel is used to obtain the grayscale tracked disk from the colored track disk. The resultant grayscale disk is shown in Fig. 3(c).

Fig. 4 shows the prototypes of two different disks, designed using the proposed coded disk design above with two different values of n and N respectively. Fig. 4(a) and Fig. 4(b) show the prototype of a 3 digit 3 ary and a 2 digit 5 ary grayscale coded disk respectively. The diameters of the designed prototype disks are 6 cm and 4 cm respectively. The two manufactured disks will be used to compare the resolution and the variation of diameter with the variation of n and N values.

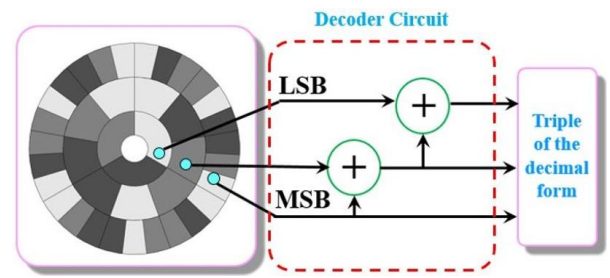


Fig 5. Decoding method of the n -digit N -ary gray code

3.3. Decoding principle

The decoder circuit for the disk designed using the affine n -digit N -ary code is shown in Fig. 5. As shown in the Fig. 5, the decoder circuit consists of simple adders. The small circles over the coded disk denote the position of the light source and photodetectors. The information obtained from the photodetectors are passed to the detector circuit. The bits are introduced into the decoder circuit starting with MSB to LSB. The decoder circuit outputs are obtained as triplets. The triplets are further processed in the decimal form using the data acquisition circuit

4. Experimental Validation

4.1. Prototype of the encoder system

The coded disks shown in Fig. 4 are used with the light source and photodetector to design the overall encoder system. The whole encoder system is shown in Fig. 6(a). As shown in the Fig. 6(a), white light emitting diodes (LEDs) are used as the light emitters. The white light passes through the transparent grayscale coded disks shown in the Fig. 4. The lights with different intensities fall on the light dependent resistors (LDRs) which are used as the photodetectors. For 2 digit 5 ary coded and 3 digit 3 ary coded disks two and three light detectors are used respectively. Fig. 6(a) is the graphical abstract of the encoder system, designed using the Solidworks. For the laboratory experiment purpose, the designed system is shown in Fig. 6(b).

The characteristic of the LDR to change its resistance with the variation of light intensity and color is used to measure the output voltage across the LDR. The characteristic of LDR is shown in Fig. 7. With the variation of illumination, the resistance of LDR changes exponentially. As a result of that, the output voltage across the LDR terminal also changes. To process and condition the output of the LDR, it is passed through the circuit shown in Fig. 8. The signal conditioning circuit consists of a differential amplifier, an inverting amplifier, span adjustment circuit and a zero adjustment circuit. The LDR is placed in a voltage divider circuit. The output of the

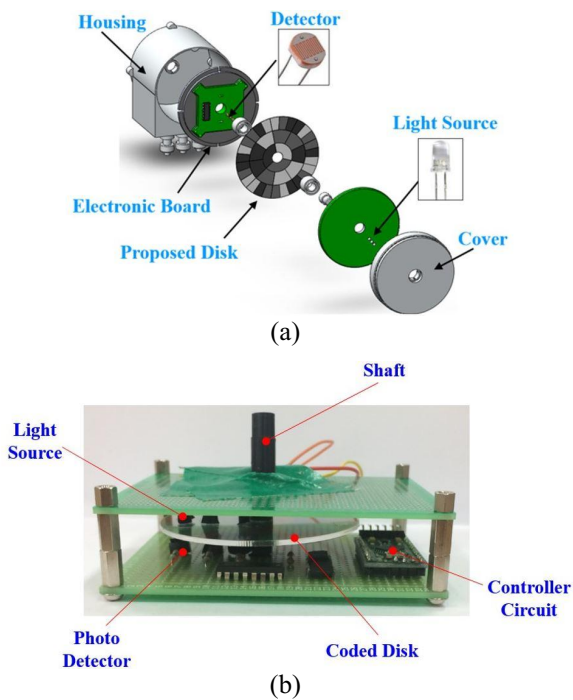


Fig. 6. (a) The graphical abstract of the overall encoder system prototype with the light source and the photodetectors (b) real prototype for the experiment purpose

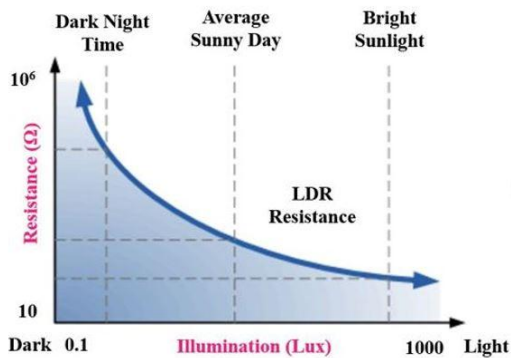


Fig. 7. The overall encoder system prototype with the light source and the photodetectors [22]

LDR fluctuates with the variation of the surrounding light and the temperature. So the output from the LDR is fed to a buffer which compensates the voltage loss. The output of the buffer is amplified using the differential amplifier. If the output of the differential amplifier has negative value, it is changed to positive value using the inverting amplifier. The output is limited to a required limit by the span adjustment circuit. The final output obtained is fed to the decoder circuit mentioned in Fig. 5.

4.2. Process of the data acquisition of the encoder system

The final output from the decoder is analyzed using

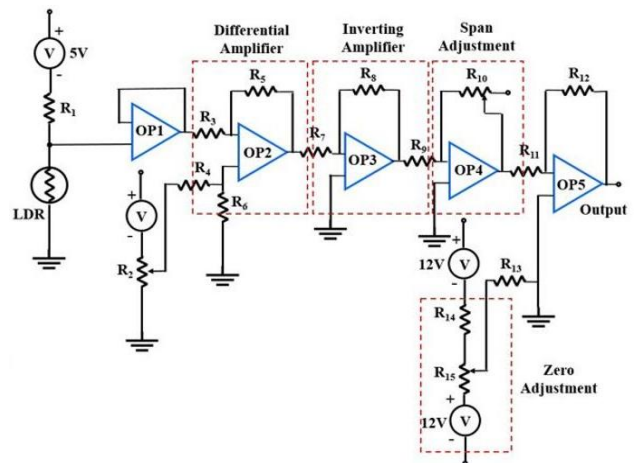


Fig. 8. Signal conditioning circuit for a single photo detector [23]

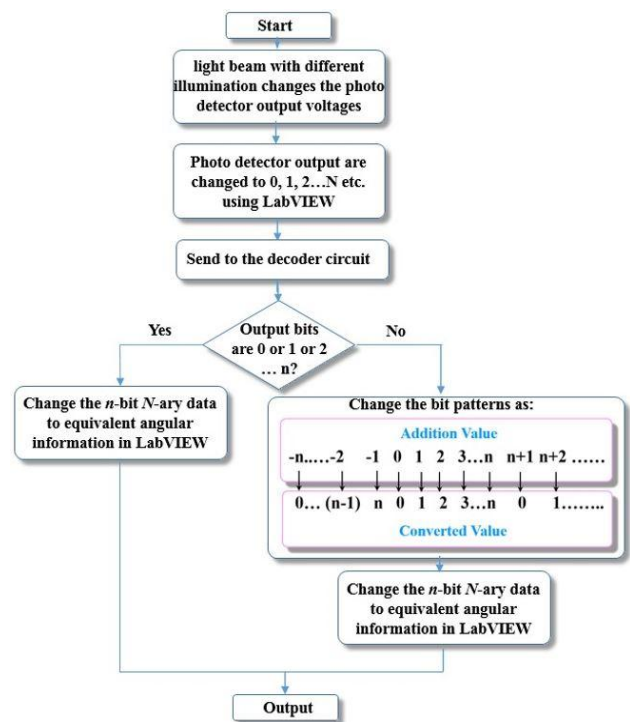


Fig. 9. The overall encoder system operation flowchart

LabVIEW. The flowchart shown in the Fig. 9 describes the steps involved in the data acquisition system. The flow chart is designed for the optical encoder systems with the two different disks shown in Fig. 4. For 3 digit 3 ary coded disk encoder system, the three different voltage outputs from the LDR assemblies is converted into 0, 1 or 2 before fed to the decoder circuit. As the decoder circuit consists of adders, for a 3 digit 3 ary system the minimum and maximum outputs of the decoder circuit are 0 and 6. But a 3 digit 3 ary system can only accommodate 0, 1 and 2. Therefore, the higher terms except {0, 1, 2} are converted to {0, 1, 2} as shown in Fig. 9. In the case of 2 digit 5 ary coded disk encoder system similar principle is

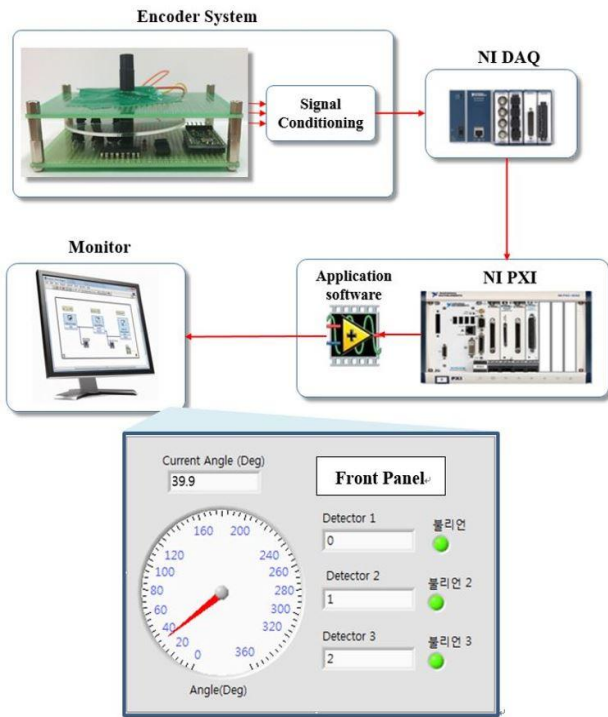


Fig 10. Experiment setup

followed, as shown in Fig. 9. In general, for n -digit N -ary gray code, if the output bit is greater than the bits present within the string $\{0, 1, 2, \dots, n\}$ of the N -ary system, from the $n+1$ bit onwards, the bits are transformed into $\{0, 1, 2, \dots, n\}$. Similarly, if the bits patterns of the decoder output are negative, $\{-1, -2, \dots, -n\}$ bits are transformed as $\{n, n-1, \dots, 0\}$.

4.3. Experimental analysis

To check the effectiveness of the proposed method, the encoder system prototype shown in Fig. 6(b) is connected to the supply and the data acquisition circuit as shown in Fig. 10. The variation of the bit pattern of the photodetector systems for both the coded disks are shown in Fig. 11. In Fig. 11(a), the output of the three photodetectors with respect to the movement of the 3 digit 3 ary gray scale coded disk are plotted. The plots show the variation of the voltage levels with respect to the change of the patterns of the grayscale coded disk. The equivalent 3 digit 3 ary code and the respective angular distances corresponding to the different photodetector voltage levels are shown in the Fig. 11(a). Similarly, Fig. 11(b) shows the voltage output of the two photodetectors used with the 2 digit 5 ary gray scale coded disk. The final codes and the angular distances are also mentioned in Fig. 11(b). This data can further be modified using the LabVIEW platform shown in Fig. 8 and the output can directly be shown in terms of absolute angles in real time. For an example, in Fig. 8, the equivalent absolute angle of the code word "012" is shown directly on the front panel as 39.9°.

Table 3. Resolution of the n -digit N -ary gray code with the variation of n and N

$N \backslash n$	1	2	3	4	5	...	n
2	180°	90°	45°	22.5°	11.25°	...	$360^\circ/2^n$
3	120°	40°	13.33°	4.44°	1.48°	...	$360^\circ/3^n$
4	90°	22.50°	5.62°	1.40°	0.35°	...	$360^\circ/4^n$
5	72°	14.40°	2.88°	0.57°	0.11°	...	$360^\circ/5^n$
.
N	$360^\circ/N$	$360^\circ/N^2$	$360^\circ/N^3$	$360^\circ/N^4$	$360^\circ/N^5$...	$360^\circ/N^n$

4.4. Discussion

As shown above, the encoder system designed using the n -digit N -ary code can effectively detect the absolute angular position. Table 3 shows the change of the resolution of the encoder system with the variation of n and N . The designed 3 digit 3 ary and 2 digit 5 ary grayscale coded disks have resolutions of 13.3° and 14.4° respectively, whereas, to achieve approximately the same resolution using a binary gray coded encoder system, 5 bit binary gray coded disk is needed. Thus, the same resolution as that of a 5-bit binary encoder system is achieved using smaller encoder disks with fewer number of tracks. Further, if we compare a 5 digit 5 ary gray coded encoder with a traditional binary gray coded encoder of 5 bit, the resolution can be improved approximately 100 times by using the 5 digit 5 ary gray coded encoder system. From Table 3, a 5 digit 5 ary encoder system has a resolution of 0.11°. To achieve the same amount of resolution using a traditional binary gray coded encoder system, 6 extra binary gray coded tracks are needed. Simultaneously the size and weight of the overall system will increase. Also, the number of sensor heads will increase to achieve the same resolution. In general, Under the condition of an equal number of n digit, the proposed N -ary gray coded disk gives $(N/2)^n$ times better resolution compared with the traditional gray coded disk. Similarly, compared with the single track and array encoder systems shown in Fig. 1, to achieve same resolution, the proposed encoder system uses smaller disk size and less number of sensor heads to encode and decode the code word. Thus it is evident that using the proposed encoder system high resolution and miniaturization can be achieved simultaneously.

Finally, as the prototype in Fig. 6(b) is designed for the laboratory experiment purpose, the photodetectors have a delay in response time with the variation of illumination. It can be seen in Fig. 11. This problem can be eliminated by using a more advanced fast response decoder circuit. Also, the experimental prototype uses LDRs in the decoder circuit. However, without proper shielding, LDR output can vary due to the inference of the ambient light conditions. Therefore, during the experiment, the LEDs

and the LDRs are surrounded using cylindrical opaque covers colored in black. Added, the problem of the inference of the ambient light can also be eliminated by putting the whole encoder system within an outer protective casing. The above mentioned issues associated with the present decoding systems opens an advanced design prospective of a CCD (Charge couple Device) camera based decoding system, which will be presented in the future extension of the present work.

5. Conclusion

In this paper, a new type of encoder system is presented based on n -digit N -ary cyclic code. The proposed coded disk design results in miniaturization of the coded track with improved resolution compared to the conventional gray code tracks. Using the proposed method, the base and the power term of the denominator in the encoder resolution expression can be varied. In addition to that, the coded disk can easily be encoded and decoded by using cheap sensory systems and electronic circuits. In future research, a more developed photodetector system with fast response time will be designed. Also, a commercial model of the proposed system with upgraded photodetector assembly will be tested and analyzed with the motor servo control system.

Acknowledgements

This work was supported by the Korea Institute of Energy Technology Evaluation and Planning (KETEP) and the Ministry of Trade, the Industry and Energy (MOTIE) of the Republic of Korea (No. 20152020000750), the Basic Science Research Program through the National Research Foundation (NRF) of Korea funded by the Ministry of Education (NRF - 2015R1D1A1A01059637).

References

- [1] S. Setinkunt, *Mechatronics*, 1st ed. John Wiley & Sons, Inc., 2007.
- [2] S. Wekhande, V. Agarwal, "High-Resolution Absolute Position Vernier Shaft Encoder Suitable for High-Performance PMSM Servo Drives," *IEEE Transaction on Instrumentation and Measurement*, vol. 55, no.1, pp. 357-364, 2006.
- [3] W. Q. Hua, W. Y. Yuan, S. Ying and W. Y. Yuan, "A Novel Miniature Absolute Metal Rotary Encoder Based on Single-Track Periodic Gray Code," in *Proceedings of International Conference on Instrumentation and Measurement, computer, communication and control*, pp. 399-402, 2012.
- [4] E. M. Petriu, "Absolute-Type Position Transducers Using a Pseudorandom Encoding," *IEEE Transaction on Instrumentation and Measurement*, vol. 36, no. 4, pp. 950-955, 1987.
- [5] G. H. Tomlinson, "Absolute-type shaft encoder using shift register sequences", *Electron. Lett.*, vol. 23, no. 8, pp.398 -400. 1987.
- [6] Y. Matsuzoe, N.Tsuji, T. Nakayama, K. Fujita and T. Yoshizawa, "High Performace Absolute Encoder using multitrack and M-Code," *Opt. Eng.*, vol. 42, no. 1, pp. 124-131, 2003.
- [7] T. Dziwinski, "A Novel Approach of an Absolute Encoder Coding Pattern", *IEEE sensor Journal*, vol. 15, no. 1, pp. 397-401, 2015.
- [8] D. Raymond and T. Garrett, "In-circuit digital tester," U.S. Patent 4 216 539, Aug. 5, 1980.
- [9] C. C. Chang, H. Y. Chen, and C. Y. Chen, "Symbolic Gray code as a data allocation scheme for two-disc systems," *Comput. J.*, vol. 35, no. 3, pp. 299-305, 1992.
- [10] D. Richards, "Data compression and Gray-code sorting," *Inf. Process. Lett.*, vol. 22, no. 4, pp. 201-205, 1986.
- [11] C. Faloutsos, "Gray codes for partial match and range queries," *IEEE Trans. Softw. Eng.*, vol. 14, no. 10, pp. 1381-1393, Oct. 1988.
- [12] I. N. Suparta and A. J. van Zanten, "Balanced maximum counting sequences," *IEEE Trans. Inf. Theory*, vol. 52, no. 8, pp. 3827-3830, 2006.
- [13] Y. Zhou, K. Panetta and C. L. Philip Chen, "(n, k, p)-Gray Code for Image Systems", *IEEE Transaction on Cybernetics*, vol. 43, no. 2, pp.515-529, 2013.
- [14] S. Erturk, "Locally refined Gray-coded bit-plane matching for block motion estimation," in *Proceedings of 3rd ISPA*, vol. 1, pp. 128-133, 2003.
- [15] C. Savage, "A survey of combinatorial Gray codes," *SIAM Rev.*, vol. 39, no. 4, pp. 605-629, 1997.
- [16] M. Flahive and B. Bose, "Balancing Cyclic R-ary Gray Codes," *The Electronics Journal of Combinatorics*, vol. 14, no. R31, pp. 1, 2007.
- [17] E. Abbena, S. Salamon, A. Gray, *Modern Differential Geometry of Curves and Surfaces with Mathematica*, 2nd ed. CRC press, 1997, pp.130.
- [18] M. Cohn, "Affine m-ary Gray Code," *Information and Control*, vol.6, pp. 70-78, 1987.
- [19] D. F. Rogers and J. A. Adams, *Mathematical Elements for Computer Graphics*, 2nd Ed., McGrawHill, New York, 1990, Chapter2.
- [20] Y. Zhao and B.Yuan, "A New Affine Transformation: Its Theory and Application to Image Coding," *IEEE Transaction on Circuits and system for video technology*, vol. 8, no. 3, pp. 269-274, 1998.
- [21] K. He1, Z. Yuan and C. Mu, "A New Affine Transformation Parameters Estimation Method", in *Proceedings of Seventh International Conference on Natural Computation*, pp. 28-32, 2011.
- [22] S. Paul and J. Chang, "Design of Absolute Encoder

Disk Coding Based on Affine n-digit N-ary Gray Code,” in *Proceedings of I2MTC*, pp. 336-341, 2016.

[23] R. L. Boylestap, “Introductory Circuit Analysis,” 10th ed. Prentice Hall, 2003.

[24] W. H. Hayt, J. E. Kemmerly and S. M. Durbin, “Engineering Circuit Analysis,” 6th ed. McGraw Hill, 2002.

on *Industrial Electronics*, and *Ieee Transactions on Superconductivity*.



Sarbajit Paul received the B.Tech. degree in electrical engineering from the School of Electrical Engineering, KIIT University, Bhubaneswar, India, in 2013, and the M.Sc. degree in electrical engineering from the Department of Electrical Engineering, Dong-A University, Busan, South Korea, in

2016, where he is currently pursuing the Ph.D. degree in motor design and control with the Mechatronics System Research Laboratory, Department of Electrical Engineering. He was a Korean Government Research Scholar under the sponsorship of National Institute of International Education, Ministry of Education, South Korea, with Mechatronics System Research Laboratory, Dong-A University from 2014 to 2016. His current research interests include motor design and drive, and instrumentation and measurement.



Junghwan Chang received the B.S. and M.S. degrees in electrical engineering and the Ph.D. degree in precision mechanical engineering from Hanyang University, Seoul, South Korea, in 1994, 1997, and 2001, respectively. From 2001 to 2002, he was with the Institute of Brain Korea 21, Hanyang University,

where he developed micro drive and high-speed spindle motor. From 2002 to 2003, he was a Research Fellow with the University of California at Berkeley, Berkeley, CA, USA, where he analyzed and developed electrically controlled engine valve system. From 2003 to 2009, he was a Technical Leader with the Korea Electrotechnology Research Institute, South Korea, where he was involved in the developments of special purpose machines. Since 2009, he has been an Associate Professor with the Department of Electrical Engineering, Dong-A University, Busan, South Korea. His current research interests include the design and analysis of electromechanical systems, such as electrically driven machine tools and magnetic gear. Dr. Chang is a member of The Korea Institute of Electrical Engineers, South Korea. He was a Steering Committee Member and the Technical Program Chair in different conferences, such as the IEEE ITEC Asia-Pacific 2016 and ICEMS 2013. He is a Reviewer of IEEE Transactions on Magnetics, Ieee Transactions on Industrial Application, Ieee Transactions